Journal of Hazardous Materials 197 (2011) 424–429

Contents lists available at SciVerse ScienceDirect

Journal of Hazardous Materials

journal homepage: www.elsevier.com/locate/jhazmat

Short communication

Electrochemical study of nitrobenzene reduction on galvanically replaced nanoscale Fe/Au particles

Zhe Chen, Zi Wang, Deli Wu*, Luming Ma

The National Engineering Research Center for Urban Pollution Control, Tongji University, 1239 Siping Road, Shanghai, 200092, China

ARTICLE INFO

Article history:
Received 3 May 2011
Received in revised form
12 September 2011
Accepted 14 September 2011
Available online 17 September 2011

Keywords:
Galvanic replacement
Electrocatalyst
Nitrobenzene
Electrochemical reduction

ABSTRACT

Nanoscale Fe/Au particles were fabricated on glassy carbon substrates by electrodeposition of Fe and the subsequent galvanic replacement with Au. The particles were characterized by scanning electron microscopy and transmission electron microscopy, and a hollow structure was found. The process and mechanism of electrochemical reduction of nitrobenzene on Fe/Au particles were studied by cyclic voltammetry and constant-potential electrolysis. The results showed that nanoscale Fe/Au particles exhibited higher catalytic activity than bulk gold for nitrobenzene reduction. Nitrobenzene reduction proceeded following different pathways with different electrolyte compositions. The removal rate of nitrobenzene on nanoscale Fe/Au particles was up to 97% with electrolysis within 120 min at −0.35 V in 0.1 M H_2SO_4 and aniline was found to be the electrolysis product.

1. Introduction

Nitrobenzene (NB) is an important raw material and solvent in the manufacturing of aniline, dye, pesticide, explosives, and pharmaceuticals [1]. A large amount of NB has been released into the environment annually due to excessive use and improper handling of the wastewater [2]. Because of the toxicity on human and the environment, NB has been listed as one of the 129 priority pollutants by USEPA and its maximum permissible concentration for wastewater is 1 mg/L [3].

Nitrobenzene is very stable due to its structure and chemical properties. The electron withdrawing group – NO_2 attached to the benzene ring makes it more difficult to be oxidized than to be reduced [4]. Therefore, more effort has been focused on the reductive approaches over the past decades, such as physical adsorption, biological reduction, chemical reduction and electrochemical reduction [5–8]. Electrochemical reduction method has received much attention, because it is cleaner, more efficient and compact, and the cost is comparable with other techniques [9]. NB reduction by electrochemical method has been extensively investigated and several electrode materials have been evaluated for their potential use in NB reduction [10–12]. Current research focused more on developing novel materials for lowering the overpotential of NB reduction to aniline (AN) [13]. It has been reported that NB reduction resulted in a variety of products via various pathways depending on the electrode and electrolyte applied. Among those products, AN was reported to be of lowest toxicity and a more favorable end product.

Nanoscale particles were extensively studied due to their special chemical and physical characteristics from the bulk state. NB reduction by metallic nanoparticles has been explored over a wide range of different materials, like Cu nanospheres [14] and nanoscale Fe^0 [15]. Moreover, mixed-metal systems often bring about a superior catalytic activity over their single-metal counterparts. For example, Dong and coworkers reported a significant enhancement in the catalytic reduction of para-nitrochlorobenzene by Pd/Fe nanoparticles. Both of the reductive amination and dechlorination products were detected due to the effect of Pd, while dechlorination product was almost undetected for the unpalladized Fe nanoparticles [16]. In fact, nitrobenzene reduction by metallic nanoparticles usually took place under open circuit conditions, and some of the particles cannot be reused after the reduction in most cases. Under some circumstances, the reaction still needs to be operated under rigorous conditions. Recently, metallic nanoparticles made by the galvanic replacement approach has gained much attention, because that it minimizes the amount of expensive metal used and leads to a larger surface area and porosity [17]. Noble metal nanoparticles have been fabricated and investigated for their catalytic ability in many aspects [18–20]. However, previous studies focused more on their applications in fuel cell or sensor, and little concerned with the their potential use as electrocatalyst in the treatment of hazardous pollutants. The transformation and electrochemical behavior of some environmental pollutants on some noble metal nanoparticles remain unknown. In the present study, nanoscale

* Corresponding author. Tel.: +86 21 65984569; fax: +86 21 65983602.
E-mail addresses: wdli101@126.com, wudeli@mail.tongji.edu.cn (D. Wu).

0304-3894/$ – see front matter © 2011 Elsevier B.V. All rights reserved.
doi:10.1016/j.jhazmat.2011.09.054

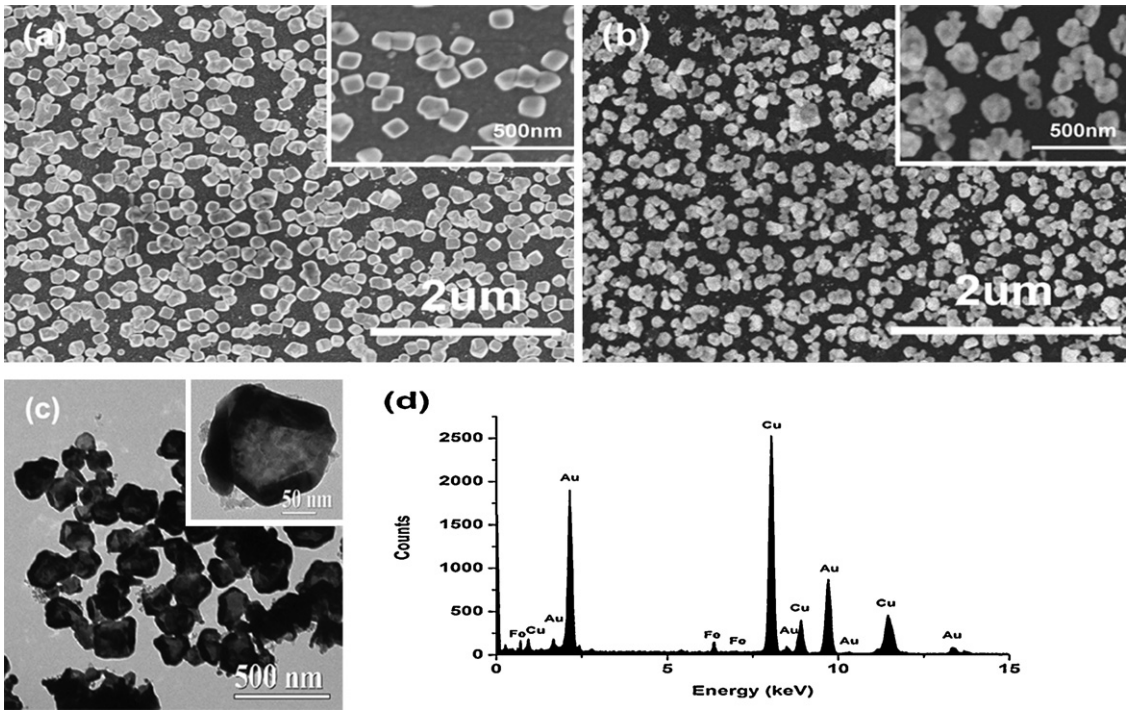

Fig. 1. SEM images of Fe particles (a) before and (b) after galvanic replacement with Au. (c) TEM images of Fe/Au particles. (d) EDX spectra of Fe/Au particles.

Fe/Au particles were fabricated through cyclic voltammetric deposition of Fe followed by a galvanic replacement reaction with Au. The surface properties of Fe/Au particles were characterized by scanning electron microscopy (SEM) and high-resolution transmission electron microscopy (HRTEM). The electrochemical behavior of NB on Fe/Au particles was studied using cyclic voltammetry and constant-potential electrolysis to provide information for the possible application of Fe/Au particles for NB reduction.

2. Experimental

All the chemicals were of analytical grade and used without further purification. All aqueous solutions were prepared with ultra-pure water (resistivity > 18.2 MΩ). Glassy carbon (GC) electrode and bulk gold electrode were 5 mm in diameter (geometric area = 0.196 cm^2). Before use, the electrodes were polished with emery paper and different sizes of alumina powders (1.0, 0.3, 0.05 μm) to a mirror-like surface, and then sonicated with ultrapure water. The Fe particles were electrodeposited on to the surface of GC electrode from deoxygenated 0.1 M Na_2SO_4 containing 20 mM $FeSO_4$ (pH 3.0–3.5). A cyclic voltammetry program was applied from −0.95 V to −1.25 V (vs. SCE) at a scan rate of 0.025 V s^{-1} for 10 cycles. After electrodeposition, the electrode was rinsed by ultrapure water and subsequently immersed in the 1 mM $HAuCl_4$ solution for 30 min. Since the standard potential of Fe^{2+}/Fe (−0.440 V vs. SHE) is lower than that of $Au(III)Cl_4^-$/Au (+1.002 V vs. SHE), Fe was spontaneously replaced by Au.

Cyclic voltammetry and constant-potential experiments were carried out by a CHI 760D electrochemical workstation at room temperature (~25 °C). A conventional three-compartment electrochemical cell with an effective volume of 40 mL (25 mL solution was used for each experiment) was used. A bright platinum plate (1 cm × 1 cm) and a saturated calomel electrode (SCE) were served as counter electrode and reference electrode, respectively. And the potentials reported in the paper were referred to SCE. All of the electrolytes were deoxygenated by extra pure nitrogen gas for 30 min before the addition of NB and a constant flow of nitrogen was maintained above the solution during experiments.

The concentration of NB and its electrolysis products were analyzed by high-performance liquid chromatography (HPLC) on a Agilent 1200 HPLC system (Agilent, USA) equipped with a reversed phase ZORBAX Eclipse XDB-C18 column (4.6 mm × 150 mm, 5 μm). A variable wavelength detector (VWD) was used for the analysis, and the detection wavelength was 254 nm for nitrobenzene and aniline. The HPLC mobile phase was the mixture of water and methanol (50:50) at a flow rate of 1.0 mL/min. Surface morphologies were observed by a S-4800 FESEM (Hitachi, Japan) and a JEM-2010 HRTEM (JEOL, Japan). The elemental composition analysis of the Fe/Au particles was performed using an Oxford energy dispersive X-ray (EDX) system attached to the HRTEM.

3. Results and discussion

3.1. Surface morphology and electrochemical behavior of the particles

Fig. 1 shows SEM images of Fe particles (denoted as Fe/GC) and Fe/Au particles (denoted as Fe/Au/GC) prepared by the method described above. As shown in Fig. 1(a), quantities of Fe particles randomly distributed over the entire glassy carbon surface with some sparse larger aggregates in some areas. The Fe particles presented a uniform cubic shape and smooth surface with size ranging from 150 to 180 nm. Fig. 1(b) depicts the micrograph of samples after galvanic replacement. The cubic-shaped Fe particles collapsed and changed into a more irregular shape, and the smooth surface became rough with small noticeable pores. However, the particle size did not change much after galvanic replacement reaction. The surface roughness resulted from the small Au nanoparticles formed outside the frame, benefiting a larger surface area and porosity. We were able to approximate the surface coverage of GC substrate based on the particle size and number as obtained by SEM analysis, with a result of 60–70%. Fig. 1(c) presents the TEM image of Fe/Au particles. As can be seen, all particles obviously had a center

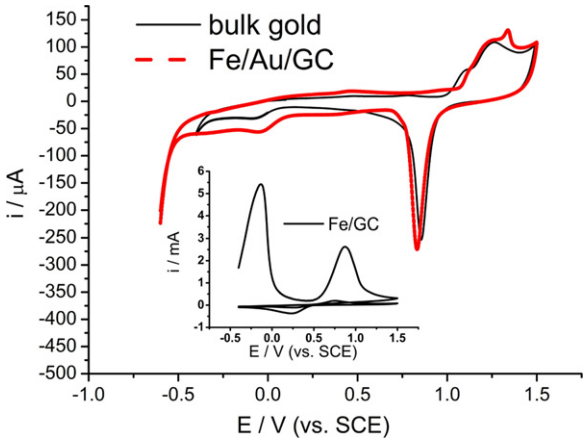

Fig. 2. CV curves of Fe/Au/GC and bulk gold in 0.1 M H_2SO_4 at scan rate 0.1 V s^{-1}. Inset is voltammogram of Fe/GC in 0.1 M H_2SO_4 at scan rate 0.1 V s^{-1}.

much brighter than the edge, confirming a hollow interior with a shell thickness of about 20 nm. The formation of the hollow structure was a result of the Kirkendall effect [21], according to which the different diffusion rates between the Fe^{2+} and $Au(III)Cl_4^-$ diffusion couple causing the formation of pores on Au shell. Oxidized Fe^{2+} ions diffused out continuously across the boundaries of the porous Au shells during the galvanic replacement reaction to form hollow Fe/Au particles finally. The chemical composition of the as-prepared Fe/Au particles was determined by EDX analysis, for which a spectrum is shown in Fig. 1(d). As expected, the presence of Fe and Au was confirmed where a Fe:Au ratio of 5:95 was found. The Cu signals were attributed to the HRTEM grid used. This high Au coverage indicates a fast metal exchange process.

The electrochemical characteristics of the Fe/Au/GC electrode with comparison to bulk gold were investigated in 0.1 M H_2SO_4. As seen in Fig. 2, the typical electrochemical behavior of bulk gold can be observed on Fe/Au/GC electrode, which is featured by the oxide formation and stripping peak at around 1.2 V and 0.8 V, respectively. The active surface area of the electrode could be determined by the charge corresponding to the stripping of the Au oxide using a reported value of 400 μC cm^{-2} [22]. An active surface area of 0.6511 cm^2 was calculated for Fe/Au/GC, smaller than that of bulk gold, which was 0.8225 cm^2. The smaller active surface area might due to the incomplete coverage of the GC electrode by Fe/Au particles. It is worth to mention that, there were significant differences between the Fe/Au/GC and the bulk gold electrodes in the double layer region. The premonolayer oxidation response was much higher on Fe/Au/GC electrode as some hydrous oxide species constructed in the form of $[Au_2(OH)_9]^{3-}$ [23]. For comparison, CV diagram of Fe/GC electrode in 0.1 M H_2SO_4 was also studied (Fig. 2 inset). Clearly, the CV diagram of Fe/Au/GC did not show much feature of Fe. Combining the TEM, EDX and CV results, it implies that the hollow-structured particles might have a double-layered bimetallic shell of Au as the over-layer and the residual Fe as the under-layer. Thus, the remaining Fe was fully protected by the Au over-layer although some of the particles were dissolved during electrochemical treatment. This kind of bimetallic hollow structure often show some electronic and chemical properties that are quite different from the monometallic state and is beneficial for an enhanced catalytic ability [24]. The electronic environment of the metal surface is changed because of the formation of the heteroatom bonds, and leads to modifications of its electronic structure through the ligand effect and consequently, its chemical properties [25]. Furthermore, the strain effect caused by the changes in orbital overlap could also affect the electronic structure [26]. Such electronic interaction between metal surfaces has been extensively studied using density functional theory (DFT) [25,27]. According to DFT, the d-band center (which is the average energy of d-band) of metal is an useful parameter, which can be used to evaluate the chemical reactivity of a certain metal and also the electronic interaction of two metals. As calculated by Ruban et al. using DFT, the d-band center of bimetallic Fe/Au was lower than that of Au, indicating a lower affinity of the metal for adsorbates (O, CO, H, etc.) [28]. This might help to explain different chemical activities for Fe/Au nanoparticles and bulk gold.

3.2. Electrochemical reduction of NB in different electrolytes

The electrochemical reduction of NB on Fe/Au/GC electrode in different electrolyte compositions was studied. As shown in Fig. 3(a), the reduction of NB started at around 0 V in 0.1 M H_2SO_4 solution (pH 1.04), with two cathodic peaks (peak 1A and peak 1B) occurred at −0.1 V and −0.33 V, attributing to NB reduction to phenylhydroxylamine (PHA) and PHA further reduction to AN, respectively. An anodic peak appeared in the return cycle at 0.32 V (peak 1C), and it was coupled with the cathodic peak (peak 1D) at 0.29 V evolving from the second scan. They represented the two-electron reversible transformation between PHA and nitrosobenzene (NSB). There was a small cathodic pre-wave at around 0.03 V that can be found only in the first scan on Fe/Au/GC, which might be ascribed to some adsorbed species on the electrode surface. The result was similar with other researchers' work, in which they found the similar pre-wave feature on Au (2 1 0) single crystal electrode after they studied a series of different gold electrodes. This might indicate that Fe/Au nanoparticles are

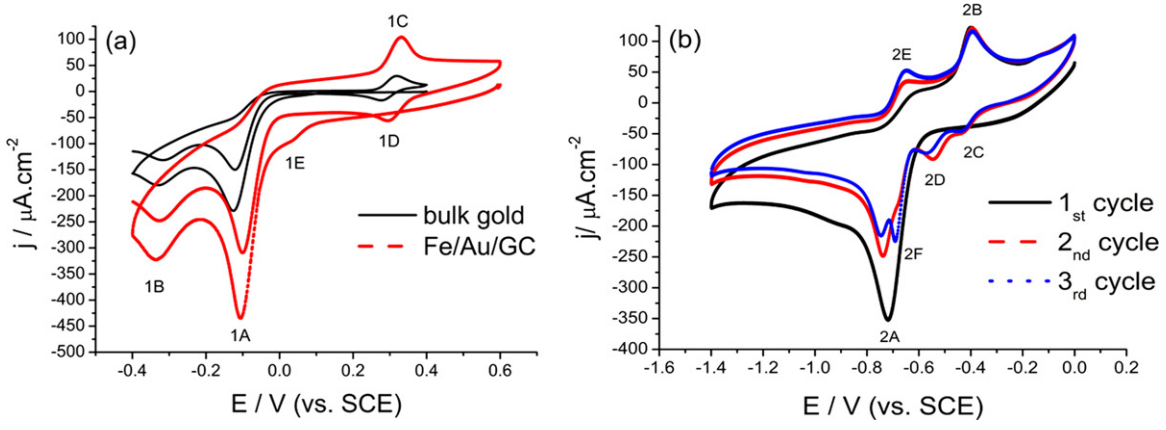

Fig. 3. (a) CV curves of Fe/Au/GC and bulk gold in 0.1 M H_2SO_4 in the presence of 1 mM NB. (b) CV curves of Fe/Au/GC in 0.1 M NaOH with 1 mM NB.

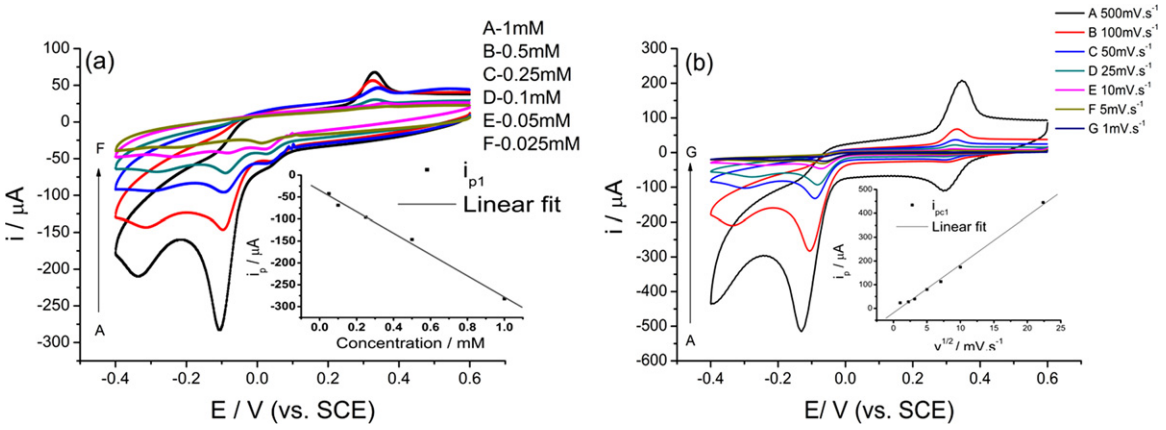

Fig. 4. (a) CV curves of Fe/Au/GC in 0.1 M H_2SO_4 at various NB concentrations. Inset is the NB reduction peak current at −0.1 V as a function of NB concentration. (b) CV curves of Fe/Au/GC in 0.1 M H_2SO_4 with 1 mM NB at different scan rates. Inset is the NB reduction peak current as a function of scan rate.

constructed by Au (2 1 0) facets which have relatively open surface. Such open surface structure is expected to exhibit a higher catalytic activity. To verify the assumption, NB reduction was also studied on bulk gold electrode. As can be seen in Fig. 3(b), the two corresponding reduction peaks (peak 1A and peak 1B) negatively shift to −0.13 V and −0.35 V, respectively. The current was normalized to surface area to compare the electrocatalytic ability. The peak current density of NB reduction on Fe/Au/GC electrode was higher than that on bulk gold. This indicates that Fe/Au nanoparticles have enhanced electrocatalytic activity than bulk gold electrode. A good explanation for the enhanced activity might be the electronic effect of the two metals. As the chemisorption of NB might also be involved in the reaction, the interaction between the d-band orbitals of the surface sites with the molecular orbitals of reactants should not be neglected [29]. It was found that surfaces with weaker molecule/surface interactions with the adsorbates demonstrate an increased activity and lower activation barrier for the hydrogenation reaction [29]. In another scenario, the galvanic replacement may lead to a rearrangement of the atoms, and generate more active sites for the chemsorption of reactants in consequence. Other possible explanation for the enhanced catalytic activity bimetallic systems involves the occurrence of mixed-sites. A mixed-site is an active site where both components of the bimetallic system participate in the catalytic transformation and shows a higher catalytic activity [26]. The synergistic effects in such sites had been observed for C_2H_6 hydrogenolysis in mixed Pd–Ni sites. However, the electroreduction of NB only occurred at the electrode surface. As for the Fe/Au nanoparticles, the electrode surface was mainly constructed by Au over-layer. Thus, the mixed-site effect might not be the main reason for the enhanced catalytic activity.

In 0.1 M NaOH alkaline solution (pH 12.87), the reaction mechanism was quite different and more complicated. As depicted in Fig. 3(b), only one single cathodic peak (peak 2A) at −0.72 V could be observed in the first scan, which was quite different from acid solution, representing the direct four-electron reduction of NB to PHA. It was reported that, the first step of nitrobenzene reduction in alkaline solutions often involved with the formation of nitrobenzene radical anion which can be either protonated or reduced to the dianion. Thus, peak 2A would be split into two closely peaks representing this two-step reaction. However, only one single peak can be observed due to the high reactivity and unsteady properties of the nitrobenzene radical. The two consecutive peaks at −0.45 V and −0.55 V (peak 2C and peak 2D) formed from second negative-going scan were identified with a two-step reaction, which was a one-electron reduction of NSB to nitrosobenzene radical anion and a further one-electron reduction to PHA. A new anodic peak at −0.65 V (peak 2E) from second positive-going scan was found to be associated with the cathodic peak at −0.69 V (peak 2F) from third scan as a result of ring coupling reaction of NSB and PHA. It was identified with the redox couple of azobenzene and hydrazobenzene.

3.3. Effect of NB concentration and scan rate

Fig. 4(a) shows the NB concentration effect on the reduction reaction as measured by cyclic voltammetry (first cycle) on Fe/Au/GC electrode. As can be witnessed, NB reduction started almost at the same potential within the investigated concentration range. The current increased at a faster speed and the NB reduction peak potential shifted towards the more negative direction with the increase of NB concentration, meanwhile the reduction peak current increased to some extent. At lower concentrations (<0.5 mM), the pre-wave gradually became a separate peak and nearly overlapped the first cathodic peak when the concentration was decreased to 0.025 mM. The change of reduction peak current at around −0.1 V with NB concentration was also plotted (Fig. 4(a) inset). A good linear relationship with a R value of 0.9966 suggests the reaction could follow zeroth order kinetics with respect to NB concentration. The limited active surface area might be the key factor that involved.

Fig. 4(b) gives NB reduction on Fe/Au/GC at various scan rates. As can be found, the curves showed two irreversible cathodic reduction peaks at all scan rates; both of the two reduction peaks shifted towards the positive direction with the decrement of peak current (denoted as i_{pc}) as the scan rate slowed down. The effect of $v^{1/2}$ on i_{pc1} was depicted in inset of Fig. 4(b), clearly. The current function correlated linearly with the square root of the scan rate. This indicates that the electrochemical reduction of nitrobenzene on Fe/Au/GC is a diffusion-controlled process. However, adsorption might still play a significant role in the process.

3.4. Constant-potential electrolysis experiments

Electrochemical reduction of NB was performed in constant-potential mode to compare the NB reduction rate of the materials by controlling the potential at −0.35 V in 0.1 M H_2SO_4 solution with an initial NB concentration of ~60 mg/L. The surface loading was calculated as NB concentration to electrode surface area ratio with a result of 306 mg/(L cm^2). The real-time current showed that the current reached steady state within 50 s and gradually went down with the depletion of NB. The steady-state current density acquired on Fe/Au/GC electrode was larger than that on bulk gold electrode.

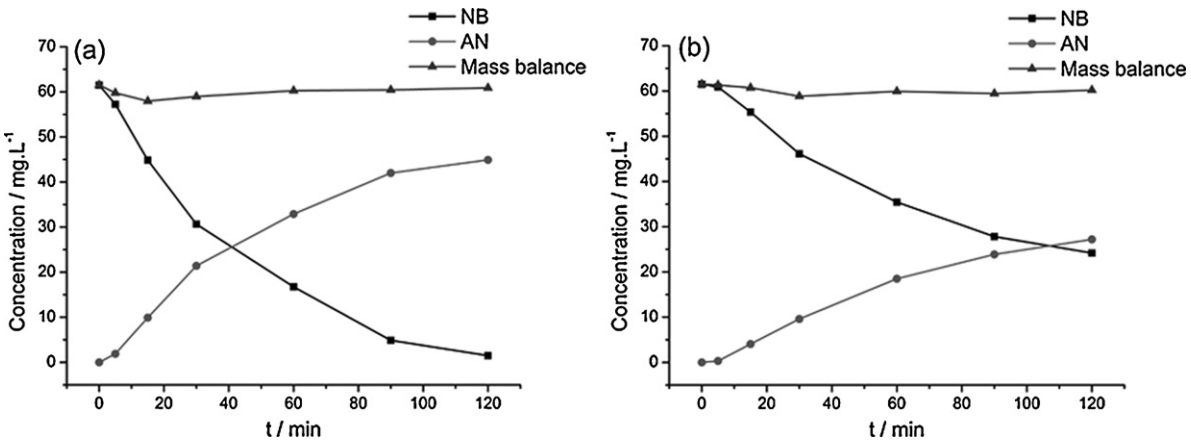

Fig. 5. NB concentration and product yield vs. time on (a) Fe/Au/GC electrode and (b) bulk gold electrode.

Fig. 5 gives the result of NB concentration before and after constant-potential electrolysis. As can be seen, nearly 75% of the NB was reduced rapidly within the first 60 min and the removal of NB was up to 97% after 120 min electrolysis with the main product of AN. However, only 59% of NB was removed after 120 min electrolysis on bulk gold electrode. Compared with bulk gold electrode, the removal rate of NB was much higher on Fe/Au/GC electrode. The results confirmed that the electrochemical reduction of NB is much faster on Fe/Au/GC than that on bulk gold electrode.

3.5. Recycling use performance

To evaluate the recycling use of the Fe/Au/GC electrode, the day-to-day stability was investigated for 30 days by conducting the CV test for 10 cycles in the 0.1 M H_2SO_4 solution containing 1 mM NB each day. The variation of peak current density and peak potential corresponding to the two NB reduction peaks (see Fig. 3(a), peak 1A and peak 1B) were depicted in Fig. 6. As shown, the peak current density for NB reduction gradually went down, with the deviation for peak potential within 0.01 V. The relative standard deviation (RSD) for peak current density was less than 10%. The Fe/Au/GC electrode suffered from little catalytic ability loss after 30 days' test, while a longer term performance remained to be investigated. And the improvement of the adhesion strength of the particles requires more effort in view of possible application of the Fe/Au particles.

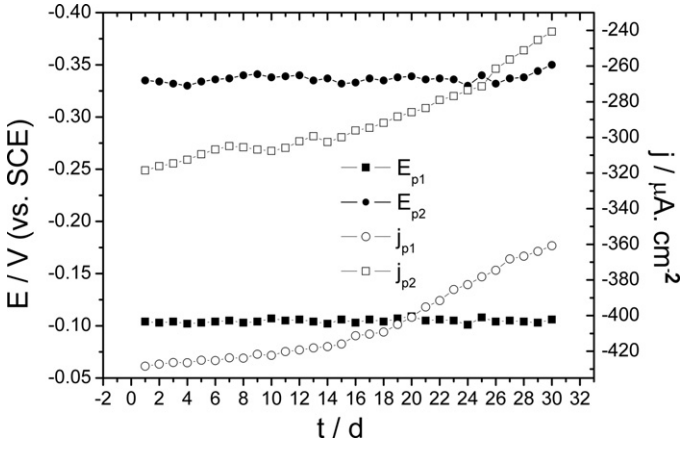

Fig. 6. Peak current density and peak potential variation as a function of time for a 30-day duration (the data were for first cycle).

4. Conclusions

Nanoscale Fe/Au particles consisting of a double-layered shell of a Au over-layer and a Fe under-layer were successfully prepared by galvanic replacement approach on glassy carbon substrates, which were characterized by SEM, TEM and EDX. When applied as an efficient catalyst for the electrochemical reduction of NB to AN, Fe/Au particles exhibited higher catalytic activity in both short-term voltammetric and medium-term potentiostatic experiments, as compared with bulk gold electrode. The removal of NB was up to 97% within 120 min electrolysis with the Fe/Au/GC electrode and the main product was AN. The superior catalytic behavior of nanoscale Fe/Au particles might be attributed to the electronic interaction of Fe and Au.

Acknowledgements

This work was supported by National Science Foundation of China (No. 50808136) and China High-tech Research and Development Plan (No. 2009AA063902).

References

[1] L. Zhao, J. Ma, Z.Z. Sun, Oxidation products and pathway of ceramic honeycomb-catalyzed ozonation for the degradation of nitrobenzene in aqueous solution, Appl. Catal. B – Environ. 79 (2008) 244–253.
[2] P.S. Majumder, S.K. Gupta, Hybrid reactor for priority pollutant nitrobenzene removal, Water Res. 37 (2003) 4331–4336.
[3] Ambient Water Qualify Criteria, in: U.S.E.P. Agency (Ed.), Washington, DC, 1980.
[4] W. Zhang, L. Chen, H. Chen, S.Q. Xia, The effect of $Fe^0/Fe^{2+}/Fe^{3+}$ on nitrobenzene degradation in the anaerobic sludge, J. Hazard. Mater. 143 (2007) 57–64.
[5] M. Chen, L. Cui, C. Li, G. Diao, Adsorption, desorption and condensation of nitrobenzene solution from active carbon: a comparison of two cyclodextrins and two surfactants, J. Hazard. Mater. 162 (2009) 23–28.
[6] Y. Mu, R.A. Rozendal, K. Rabaey, J. Keller, Nitrobenzene removal in bioelectrochemical systems, Environ. Sci. Technol. 43 (2009) 8690–8695.
[7] R. Mantha, K.E. Taylor, N. Biswas, J.K. Bewtra, A continuous system for Fe^0 reduction of nitrobenzene in synthetic wastewater, Environ. Sci. Technol. 35 (2001) 3231–3236.
[8] G. Seshadri, J.A. Kelber, A study of the electrochemical reduction of nitrobenzene at molybdenum electrodes, J. Electrochem. Soc. 146 (1999) 3762–3764.
[9] G.H. Chen, Electrochemical technologies in wastewater treatment, Sep. Purif. Technol. 38 (2004) 11–41.
[10] Y.P. Li, H.B. Cao, C.M. Liu, Y. Zhang, Electrochemical reduction of nitrobenzene at carbon nanotube electrode, J. Hazard. Mater. 148 (2007) 158–163.
[11] C.A. Ma, S. Chen, Y.Q. Chu, X.B. Mao, Electrochemical reduction of nitrobenzene in ionic liquid BMimBF(4)-H_2O, Acta Phys. – Chim. Sin. 23 (2007) 575–580.
[12] M.C.F. Oliveira, Study of the hypophosphite effect on the electrochemical reduction of nitrobenzene on Ni, Electrochim. Acta 48 (2003) 1829–1835.
[13] C.Z. Zhang, J. Yang, Z.D. Wu, Electroreduction of nitrobenzene on titanium electrode implanted with platinum, Mater. Sci. Eng. B – Solid 68 (2000) 138–142.
[14] A.K. Patra, A. Dutta, A. Bhaumik, Cu nanorods and nanospheres and their excellent catalytic activity in chemoselective reduction of nitrobenzenes, Catal. Commun. 11 (2010) 651–655.

[15] X. Bai, Z.-F. Ye, Y.-Z. Qu, Y.-F. Li, Z.-Y. Wang, Immobilization of nanoscale Fe^0 in and on PVA microspheres for nitrobenzene reduction, J. Hazard. Mater. 172 (2009) 1357–1364.
[16] T. Dong, H. Luo, Y. Wang, B. Hu, H. Chen, Stabilization of Fe-Pd bimetallic nanoparticles with sodium carboxymethyl cellulose for catalytic reduction of para-nitrochlorobenzene in water, Desalination 271 (2011) 11–19.
[17] Y.S. Shon, G.B. Dawson, M. Porter, R.W. Murray, Monolayer-protected bimetal cluster synthesis by core metal galvanic exchange reaction, Langmuir 18 (2002) 3880–3885.
[18] Y.Y. Mu, H.P. Liang, J.S. Hu, L. Jiang, L.J. Wan, Controllable Pt nanoparticle deposition on carbon nanotubes as an anode catalyst for direct methanol fuel cells, J. Phys. Chem. B 109 (2005) 22212–22216.
[19] O.M. Wilson, M.R. Knecht, J.C. Garcia-Martinez, R.M. Crooks, Effect of Pd nanoparticle size on the catalytic hydrogenation of allyl alcohol, J. Am. Chem. Soc. 128 (2006) 4510–4511.
[20] J. Luo, P.N. Njoki, Y. Lin, L.Y. Wang, C.J. Zhong, Activity-composition correlation of AuPt alloy nanoparticle catalysts in electrocatalytic reduction of oxygen, Electrochem. Commun. 8 (2006) 581–587.
[21] Y. Yin, R.M. Rioux, C.K. Erdonmez, S. Hughes, G.A. Somorjai, A.P. Alivisatos, Formation of hollow nanocrystals through the nanoscale Kirkendall effect, Science 304 (2004) 711–714.
[22] S. Trasatti, O.A. Petrii, Real surface area measurements in electrochemistry, J. Electroanal. Chem. 327 (1992) 353–376.
[23] A.P. O'Mullane, S.J. Ippolito, Y.M. Sabri, V. Bansal, S.K. Bhargava, Premonolayer oxidation of nanostructured gold: an important factor influencing electrocatalytic activity, Langmuir 25 (2009) 3845–3852.
[24] M.R. Kim, D.K. Lee, D.-J. Jang, Facile fabrication of hollow Pt/Ag nanocomposites having enhanced catalytic properties, Appl. Catal. B – Environ. 103 (2011) 253–260.
[25] J.R. Kitchin, J.K. Norskov, M.A. Barteau, J.G. Chen, Modification of the surface electronic and chemical properties of Pt(1 1 1) by subsurface 3d transition metals, J. Chem. Phys. 120 (2004) 10240–10246.
[26] B. Coq, F. Figueras, Bimetallic palladium catalysts: influence of the co-metal on the catalyst performance, J. Mol. Catal. A: Chem. 173 (2001) 117–134.
[27] J. Greeley, J.K. Nørskov, Large-scale, density functional theory-based screening of alloys for hydrogen evolution, Surf. Sci. 601 (2007) 1590–1598.
[28] A. Ruban, B. Hammer, P. Stoltze, H.L. Skriver, J.K. Nørskov, Surface electronic structure and reactivity of transition and noble metals, J. Mol. Catal. A: Chem. 115 (1997) 421–429.
[29] J.G. Chen, C.A. Menning, M.B. Zellner, Monolayer bimetallic surfaces: experimental and theoretical studies of trends in electronic and chemical properties, Surf. Sci. Rep. 63 (2008) 201–254.